SPECTROSCOPIC ELLIPSOMETRY STUDIES ON ZINC OXIDE THIN FILMS DEPOSITED BY SOL–GEL METHOD WITH VARIOUS PRECURSOR CONCENTRATIONS

MARYAM MOTALLEBI AGHGONBAD* and HASSAN SEDGHI†

Department of Physics, Urmia University, Urmia, Iran
*m.motallebi89@gmail.com
†H.sedghi@urmia.ac.ir

Zinc Oxide thin films were deposited on glass substrates by sol–gel spin coating method. Zinc acetate dihydrate, 2-methoxyethanol and monoethanolamine were used as precursor, solvent and stabilizer, respectively. Zinc acetate dihydrate was used with different molar concentrations of 0.15, 0.25 and 0.5 M. Optical properties of ZnO thin films such as dielectric constants, absorption coefficient, Urbach energy and optical band gap energy were calculated by spectroscopic ellipsometry (SE) method. The effect of zinc acetate concentration on optical properties of ZnO thin films is investigated. ZnO thin film with Zn concentration of 0.25 M had the highest optical band gap. Wemple DiDomenico oscillator model was used for calculation of the energy of effective dispersion oscillator, the dispersion energy, the high frequency dielectric constant, the long wavelength refractive index and the free carrier concentration.

Keywords: Spectroscopic ellipsometry; sol–gel; optical properties; ZnO.

1. Introduction

Transparent conductive oxide films are used in variety of applications due to their special physical properties such as large band gaps and high optical transparency in visible spectral region.[1] ZnO is a member of transparent conductive oxides. It has a large band gap of 3.37 eV and large exiton energy of 60 meV.[2,3] Zinc oxide is a dominant material in large number of areas. ZnO is inexpensive, relatively abundant, chemically stable, easy to prepare and nontoxic.[4] ZnO thin films have attracted much attention due to their potential applications in solar cells,[5,6] gas sensors[7] and thin film transistors.[8,9] ZnO thin films have been made by variety of techniques such as RF magnetron sputtering,[10,11] DC sputtering,[12] spray pyrolysis,[13–15] pulsed

laser deposition,[16] chemical vapor deposition,[17] vacuum coating,[18] sol–gel[4,19,20] and electrochemical deposition.[21] Among these, sol–gel is simple, low cost and convenient for preparing homogeneous and smoother thin films. The properties of thin films deposited by sol–gel spin coating technique are influenced by three major parameters such as pre-coating parameters (precursor concentration, aging time), coating parameters (spin coating speed, coating time) and post coating parameters (annealing temperature).[22]

Many methods have been used to study the optical properties of ZnO thin films. Among these, spectroscopic ellipsometry[23,24] (SE) is a nondestructive method for determining such properties without the limitations of the other methods that have physical contact to the film.[23] Ellipsometry method uses

---

*Corresponding author.

M. M. Aghgonbad & H. Sedghi

detection of polarization state to characterize thin films. Due to dependence of polarization response on structure and optical properties of the films, a lot of information can be obtained using ellipsometry method.[25] In SE method, various characterizations including refractive index and dielectric constant are possible. SE has an indirect nature and requires appropriate modeling analysis to extract optical properties. The interpretation of measurement results is rather difficult from the absolute values of (Ψ, Δ). Thus, the construction of optical model is required for data analysis. Ellipsometry data analysis consists of three major parts: dielectric function modeling, construction of an optical model and fitting to measured (Ψ, Δ) spectra. The optical model should be selected according to the optical properties of the sample.[26]

In this paper, we report growth of ZnO thin films with different zinc acetate concentrations of 0.15, 0.25 and 0.5 M on glass substrate by sol–gel spin coating method. SE method was used to calculate the optical properties such as dielectric constants, absorption coefficient, Urbach energy and optical band gap energy. Also, we used Wemple DiDomenico oscillator model to calculate the energy of effective dispersion oscillator, the dispersion energy, the high frequency dielectric constant, the long wavelength refractive index and the free carrier concentration. The aim of this work is to study the effect of zinc acetate concentration on optical properties of ZnO thin films.

2. Experimental Details

In this work, zinc acetate dihydrate [$Zn(C_2H_3O_2)_2 \cdot 2H_2O$], 2-methoxyethanol ($C_3H_8O_2$) and monoethanolamine ($C_2H_7NO$) were used as precursor, solvent and stabilizer, respectively. At first, zinc acetate dihydrate was dissolved in 25 ml of 2-methoxyethanol at room temperature. Different concentrations of zinc acetate, 0.15, 0.25 and 0.5 M were used in the mixture. The mixture was stirred at $60°C$ for 1 h. During the stirring, monoethanolamine was added drop by drop until a clear solution was formed. The solution was kept at room temperature for 72 h for aging. ZnO thin films were deposited on glass substrates by spin coating at 4800 rpm. Before deposition, the substrates were cleaned in acetone, ethanol and de-ionized water. The films were preheated in air for 10 min at $200°C$. Then the films were annealed at $500°C$ for an hour.

In this work, SE 800 DUV (SENTECH) instrument with the measurement wavelength range of 300–800 nm was used for analyzing. The SE 800 DUV is applying the Step Scan Analyzer measurement mode. The measurements were done in Spectra ray software.[26] The steps of spectra ray operation are sample alignment, ellipsometric measurement, modeling, fitting and reporting.

In order to calculate the correct incidence angle and (Ψ, Δ) data, sample height and tilt aligned accurately. Then the incidence angle, the wavelength limit and the polarization position were indicated and the measurement was performed. In the modeling step in accordance with the selected material, the proper dispersion formula was used to describe the optical constants dispersion of the thin film. Then the proper model for the sample was made, fit parameters were chosen and the fitting process was done. At last properties such as dielectric constant and transmittance, were calculated.

3. Results and Discussion

3.1. *Ellipsometric measurements of dielectric constant of ZnO thin films*

SE measures the change in polarized light when it is reflected on a film or transmitted through the sample. Ellipsometry measures the two values (ψ, Δ) which represent the amplitude ratio and phase difference between p and s polarized light waves, respectively. Ellipsometric parameters (ψ, Δ) are defined from the ratio of the amplitude reflection coefficient for p and s polarizations.[5,27]

$$\rho \equiv \tan\psi \exp(i\Delta) \equiv \frac{r_p}{r_s}. \tag{1}$$

Since in SE method, instruction of an optical model is necessary and the dielectric function of the samples are not known, a model consisting of a glass substrate, ZnO thin film, surface roughness layer and air as the ambient medium (as shown in Fig. 1) was designed.

Surface roughness is modeled by a Bruggemann type effective medium approximation (EMA) with 50% of voids and 50% of ZnO. When ZnO thin film is formed on glass substrate, the effect of backside reflection leads to complications in the SE analysis. To eliminate the backside reflection, in measuring the properties of Fe-doped ZnO thin films, the rear surface of the substrates were roughened and Scotch tape was used during the measurement. In this case,
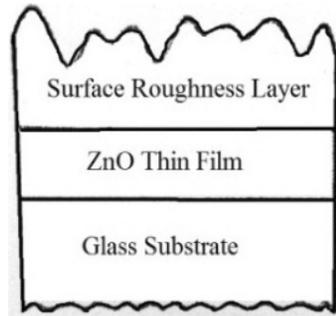
Fig. 1.   The optical model used in SE analysis.

when light enters the Scotch tape, scattering by the cloudy translucent material and backside reflections are suppressed.

In this work, Leng–Lorentz oscillator model[28] was used. SENTECH has expanded the formula published by Leng to the following form:

$$\varepsilon(E) = \varepsilon_\infty + \sum_{i=1}^{N} \left(\frac{C_{0i}}{E^2} [e^{i\beta_i}(E_{g_i} - E - i\Gamma_i)^{\mu_i} \right.$$
$$+ e^{-i\beta_i}(E_{g_i} + E + i\Gamma_i)^{\mu_i}$$
$$- 2\mathrm{Re}[e^{-i\beta_i}(E_{g_i} + i\Gamma_i)^{\mu_i}]$$
$$\left. -2i\mu_i E \,\mathrm{Im}\left[e^{-i\beta_i}(E_{g_i} + i\Gamma_i)^{\mu_i - 1}\right]\right). \quad (2)$$

For a single critical point, C_0 is the amplitude, β is the phase, μ is the order of the pole, E_g is the critical point energy and Γ is the broadening parameter of the oscillator.

In Figs. 2 and 3, the experimental and fitted ellipsometric parameters (ψ, Δ) are shown for ZnO thin films with different Zn concentrations as a function of wavelength.

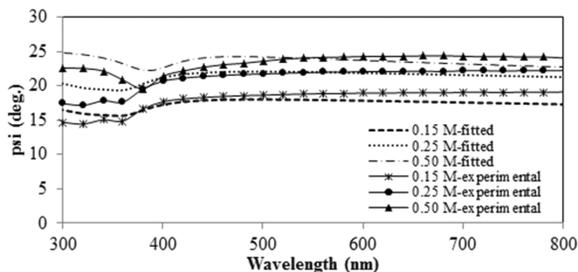To qualify the difference between the experimental and fitted data, the mean square error (MSE) was

Fig. 2.   The experimental and fitted ellipsometry parameter ψ as a function of wavelength for ZnO thin films with different Zn concentrations.
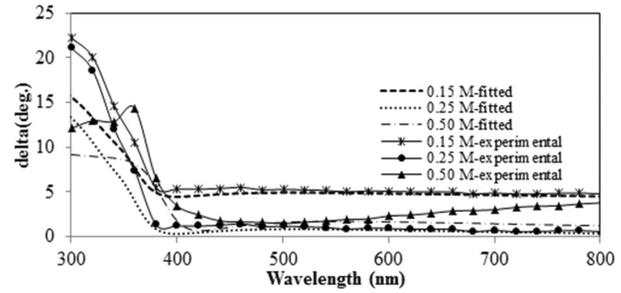

Fig. 3.   The experimental and fitted ellipsometry parameter Δ as a function of wavelength for ZnO thin films with different Zn concentrations.

Table 1.   MSE of ZnO thin films with different zinc acetate concentrations.

ZnO thin films	Zn concentration (M)	Mean square error
I	0.15	0.73
II	0.25	0.88
III	0.50	1.24

calculated by the following equation:

$$(\mathrm{MSE})\chi^2 = \frac{1}{N} \sum_{i=1}^{N} \frac{(\mathrm{Mes}_i - \mathrm{Th}_i)^2}{\sigma_i^2}, \quad (3)$$

where σ_i is the standard deviation of the ith data point, N is the number of data points, Mes_i is the ith experimental data point and Th_i is the ith calculated data point from assumed theoretical model. MSE value obtained by SE method is shown in Table 1.

When the model matches the experimental data as closely as possible, MSE exhibits a minimum value.

Figure 4 displays the real and imaginary parts of dielectric constant $(\varepsilon_1, \varepsilon_2)$, for ZnO thin films produced in this work.

It can be seen that ε_1 and ε_2 follow the same pattern and both decrease with increasing wavelength in the visible spectral range. The higher value of the real part of dielectric constant in comparison with the imaginary part shows low energy loss of light through ZnO thin films in the visible spectral range. Figure 4(a) shows that with increasing zinc acetate concentration, ε_1 decreases. It can be seen in Fig. 4(b) that there is an increment for ε_2 in the ultraviolet region and decrement in the visible region with increasing Zn concentrations.
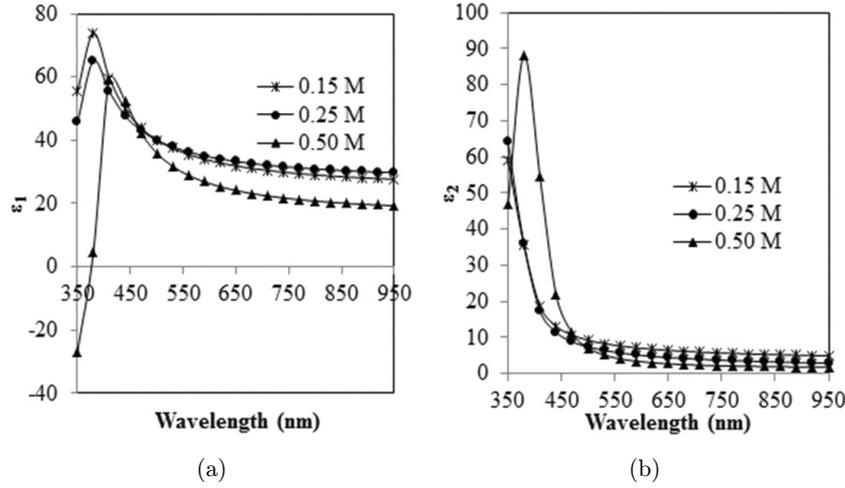
Fig. 4.   (a) Real and (b) imaginary part of dielectric function of ZnO thin films with different zinc acetate concentrations of 0.15, 0.25 and 0.5 M.

3.2.   *Zn concentration effect on Urbach energy band gap of ZnO thin films*

Figure 5 shows the absorption coefficient, (α) and the plot of $\ln(\alpha)$ vs photon energy of ZnO thin films.

After about 450 nm wavelength, by increasing zinc acetate concentration, the absorption coefficient decreases. It can be seen in Fig. 5(a) that, as Zn concentration increases, the absorption edge shifts towards higher wavelengths. The absorption edge is known as Urbach edge. The imperfection in the structurally disordered film leads to broadening the bands of localized states. In this case a band gap reduction may occur due to the Urbach edge. Near the band edge, the absorption coefficient has an exponential dependence on photon energy. This dependence is given as follows[29–31]:

$$\alpha = \alpha_0 \exp\left(\frac{E - E_0}{E_u}\right), \qquad (4)$$

where α_0, E_0 are constants, E_u is Urbach energy and E is the incident photon energy. The reciprocal of the slope of the linear region in plot of $\ln\alpha$ vs E yields the value of E_U (as shown in Fig. 5(b)). Urbach energy is the width of the tails of the localized states associated with the amorphous state in the forbidden band. Urbach energy at band edges for
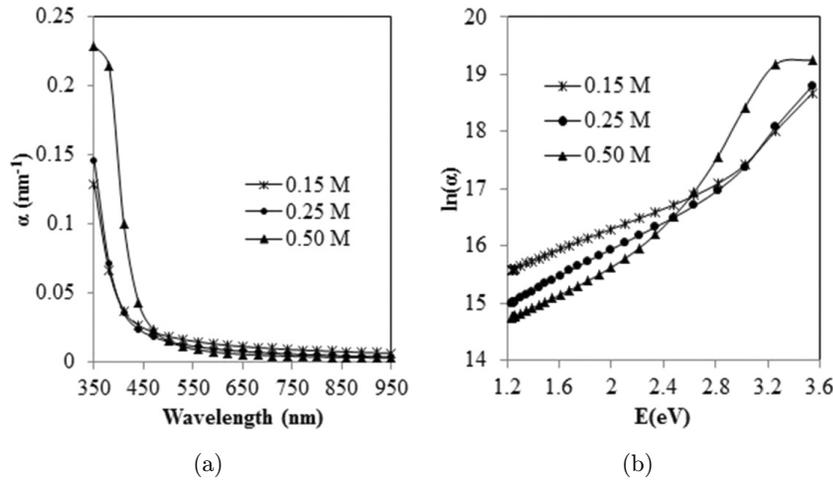

Fig. 5.   (a) Absorption coefficient and (b) Urbach energy of ZnO thin films with different zinc acetate concentrations of 0.15, 0.25 and 0.5 M.
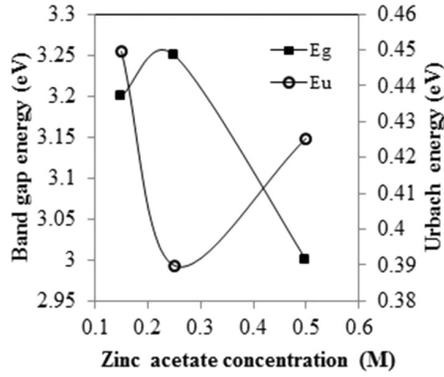
Fig. 6.   Band gap energy and Urbach energy of ZnO thin films with different zinc acetate concentrations of 0.15, 0.25 and 0.5 M.

ZnO films of different Zn precursor concentrations is shown in Fig. 5. The optical band gap energy, E_g, of ZnO thin films can be calculated by the equation below[32,33]:

$$\alpha E = A(E - E_g)^n, \tag{5}$$

where, α is the absorption coefficient, E is the photon energy, A is a constant and n is $1/2$, 2, $3/2$ and 3 for allowed direct, allowed indirect, forbidden direct and forbidden indirect band gap semiconductors, respectively. For direct band gap semiconductors such as ZnO, $n = 1/2$ is selected. The energy gap (E_g) value is calculated by extrapolation of the straight line of the plot of $(\alpha E)^2$ vs photon energy (E).

Figure 6 shows the calculated band gap energy for the layers in this work.

From Fig. 6 it could be seen that the thin film with Zn concentration of 0.25 M has the highest optical band gap and lowest Urbach energy. By increasing zinc acetate concentration to 0.5 M, band gap energy decreases from 3.25 eV to 3.0 eV. This could be due to increase in carrier concentration.
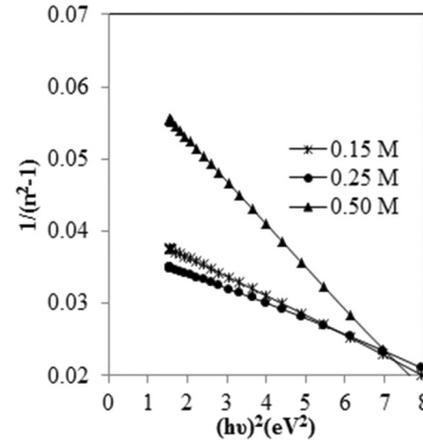

Fig. 7.   Plot of $1/(n^2 - 1)$ vs E^2 for ZnO thin films with different zinc acetate concentrations of 0.15, 0.25 and 0.5 M.

3.3. *Effect of Zn concentration on the refractive index dispersion data*

A single oscillator model suggested by Wemple and DiDomenico was used to estimate the energy band structure of ZnO thin films. In single oscillator model, the dispersion function is as follows[34–36]:

$$n^2(E) = 1 + \frac{E_0 \cdot E_d}{E_0^2 - (\hbar\omega)^2}, \tag{6}$$

where the two parameters E_0 and E_d are connected to optical properties of the thin film and are single oscillator energy and dispersive energy, respectively. n is the refractive index and $\hbar\omega$ is the photon energy. In Fig. 7 the plot of $1/(n^2 - 1)$ vs $(\hbar\omega)^2$ is shown.

The resulting straight line yields values of E_0 and E_d. In the present work, E_0 and E_d are determined from the experimental data and the results are mentioned in Table 2.

Here, E_0 is a measure of the average excitation energy for electronic transitions and E_d is a measure of the average strength of the interband optical transitions. In the layer with Zn concentration of

Table 2.   The energy of effective dispersion oscillator (E_0), the dispersion energy (E_d), the optical band gap (E_g), band gap of the single oscillator model (E_a), and the plasma oscillator energy $(\hbar\omega_p)$ of ZnO thin films with different coating speeds.

ZnO thin films	Zn concentration (M)	E_0 (eV)	E_d (eV)	E_g (eV)	E_0/E_g	E_a (eV)	$\hbar\omega_p$ (eV)
I	0.15	3.92	93.39	3.20	1.22	2.61	15.61
II	0.25	4.20	110.63	3.25	1.29	2.51	16.66
III	0.50	3.34	51.40	3.00	1.11	2.69	11.75

0.25 M, E_d has the highest value. The ordering of the film structure leads to E_d increase, so the films with Zn concentration of 0.25 M were more crystalline. The increase in E_0 values obtained for the films with Zn concentration of 0.25 M are in accordance with the increase in the optical band gap energy. E_0 has an empirical relationship with E_g. In this work, $E_0 \approx 1.2\,E_g$ is obtained. In a single oscillator model, the band gap E_a introduced by Hopfield provides the link between the single oscillator parameters (E_0, E_d) and the Phillips static dielectric constant parameters $(E_g, \hbar\omega_p)$, as follows:

$$E_0 E_a = E_g^2, \tag{7}$$

$$E_a E_d = (\hbar\omega_p)^2, \tag{8}$$

where E_g is the optical band gap energy and $\hbar\omega_p$ is the plasma oscillator energy. The calculated values of E_a and $\hbar\omega_p$ are listed in Table 2.

3.4. Effect of Zn concentration on the free carrier concentration

According to Pankove, the real part of dielectric constant is obtained by[37]:

$$\varepsilon_1 = n^2 - k^2 = \varepsilon_\infty - \left(\frac{e^2}{\pi\varepsilon_0 c^2}\right)\left(\frac{N}{m^*}\right)\lambda^2, \tag{9}$$

where ε_∞ is the high frequency dielectric constant, N is the free charge carrier concentration, ε_0 is the permittivity of the free space, e is the charge of electron, c is the velocity of light and m^* is the effective mass of the charge carriers. From linear regression of dependence ε_1 vs λ^2, ε_∞ and N can be obtained (as shown in Fig. 8).
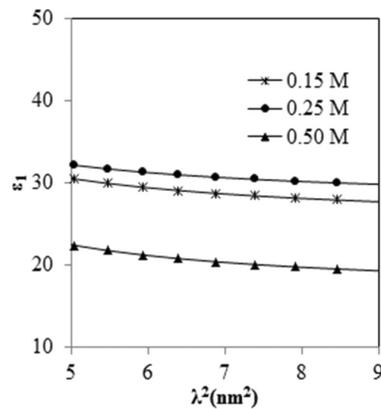
Table 3.   The high frequency dielectric constant (ε_∞), the long wavelength refractive index (n_∞) and the free carrier concentration (N) of ZnO thin films with different coating speeds.

ZnO thin films	Zn concentration (M)	ε_∞	n_∞	N (cm^{-3})
I	0.15	31	5.56	1.19×10^{20}
II	0.25	34	5.83	9.98×10^{19}
III	0.50	23	4.79	1.30×10^{20}

The calculated values of ε_∞ and N are mentioned in Table 3.

The ZnO thin films with Zn concentration of 0.25 M had the least free charge carrier concentration and the films with Zn concentration of 0.50 M had the most.

3.5. Effect of Zn concentration on static refractive index

The average interband oscillator wavelength (λ_0) and the average oscillator strength (S_0) parameters were calculated for ZnO thin films with different Zn concentrations by the following equation[37]:

$$n^2 = 1 + \frac{S_0 \lambda_0^2}{1 - \left(\frac{\lambda_0}{\lambda}\right)^2}, \tag{10}$$

S_0 and λ_0 can be evaluated from the plots of $1/(n^2 - 1)$ vs $1/\lambda^2$ (as shown in Fig. 9).

Also refractive index, n_0, can be obtained by the following relation:

$$S_0 = \frac{(n_0^2 - 1)}{\lambda_0^2}, \tag{11}$$

Fig. 8.   Plot of ε_1 vs λ^2 for ZnO thin films with different zinc acetate concentrations of 0.15, 0.25 and 0.5 M.
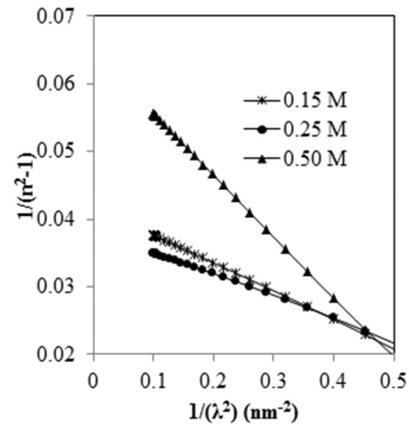

Fig. 9.   Plot of $1/(n^2 - 1)$ vs $1/\lambda^2$ for ZnO thin films with different zinc acetate concentrations of 0.15, 0.25 and 0.5 M.

Table 4.   The average interband oscillator wavelength (λ_0), the average oscillator strength (S_0), the static refractive index (n_0) and the static dielectric constant (ε_s) of ZnO thin films with different coating speeds.

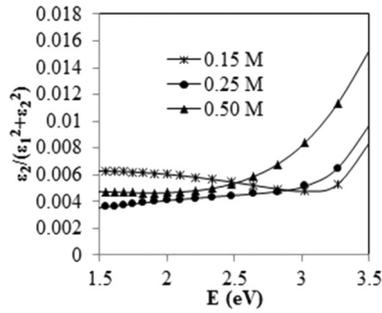| ZnO thin films	Zn concentration (M)	S_0 (nm^{-2})	λ_0 (nm)	ε_s	n_0
I	0.15	0.00024	332.22	27.48	4.05
II	0.25	0.00030	282.48	24.93	4.99
III	0.50	0.00011	374.53	16.42	5.24

Fig. 10.   Loss function of ZnO thin films with different zinc acetate concentrations of 0.15, 0.25 and 0.5 M.

where n_0 provides a good indication of the structure and density of the material. As the static refractive index (n_0) equals to $\sqrt{\varepsilon_s}$, one can obtain the static dielectric constant (ε_s). The values of S_0, λ_0, n_0 and ε_s are listed in Table 4.

3.6.   *Loss function of ZnO thin films*

The loss function curves describe the energy loss of a fast electron traveling in the material. The energy loss functions of ZnO thin films with different zinc acetate concentrations are calculated by the following equation[38]:

$$-\mathrm{Im}\,\varepsilon^{-1} = -\mathrm{Im}\left(\frac{1}{\varepsilon_1 + i\varepsilon_2}\right) = \frac{\varepsilon_2}{\varepsilon_1^2 + \varepsilon_2^2}. \qquad (12)$$

The results are shown in Fig. 10.

Theoretically, the energy loss function should exhibit a δ-like spike at the plasma frequency, ω_p, but in actual materials, due to the background and damping of single particle transitions (and other decay mechanisms), the $-1/\varepsilon$ plasma resonances are rather broad.

3.7.   *Zn concentration effect on the real and imaginary parts of conductivity*

Figure 11 displays the real and imaginary parts of conductivity (σ_1, σ_2), for ZnO thin films with different Zn precursor concentration, which are given by the following equations:

$$\sigma_1 = \frac{\varepsilon_2\omega}{4\pi}, \qquad (13)$$

$$\sigma_2 = \frac{(1 - \varepsilon_1)\omega}{4\pi}, \qquad (14)$$

where, ω, is the angular frequency. In Fig. 11(a) it is shown that by increasing Zn concentration, the real part of conductivity decreases in the visible wavelength region.

As it can be seen in Fig. 11(b) there is a peak at about 380 nm wavelengths for thin films with Zn concentration of 0.15 and 0.25 M which is shifted to

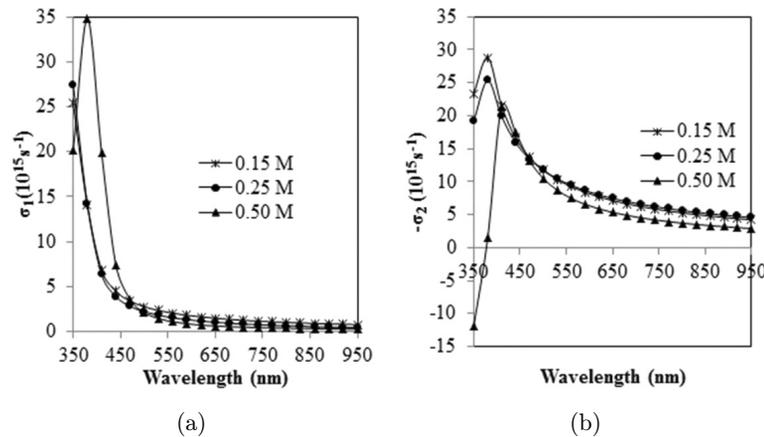(a)   (b)

Fig. 11.   (a) Real and (b) imaginary part of conductivity of ZnO thin films with different zinc acetate concentrations of 0.15, 0.25 and 0.5 M.
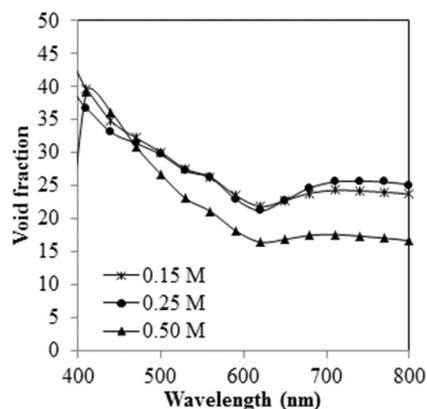
M. M. Aghgonbad & H. Sedghi

Fig. 12.   Fraction of voids for ZnO thin films with different zinc acetate concentrations of 0.15, 0.25 and 0.5 M.

wavelength of 400 nm for the layer with Zn concentration of 0.50 M.

3.8. Zn concentration effect on void fraction of ZnO thin films

The void fractions of ZnO thin films calculated for different Zn concentrations of 0.15, 0.25 and 0.50 M are shown in Fig. 12 as a function of wavelength.

In general, migration of grains should lead to a decrease in fraction of voids. With changing Zn concentration, the fraction of voids changes too. As it can be seen in Fig. 12, with increasing Zn concentration, void fraction of thin films had been decreased.

4.   Conclusion

In this work, the effect of zinc acetate concentration in the optical properties of ZnO thin films was studied. The optical properties were calculated by SE method. By choosing surface roughness/thin film/substrate as a model, the experimental and fitted parameters (ψ, Δ) were obtained. It can be deduced from the results that with increasing zinc acetate concentration, real part of dielectric constant decreases. For imaginary part of dielectric constant, there is an increment in the ultraviolet region and decrement in the visible region. The highest band gap energy and the lowest Urbach energy was obtained for ZnO thin films with Zn concentration of 0.25 M. The optical dispersions (E_0 and E_d) were also analyzed using Wemple DiDomenico. In the layer with Zn concentration of 0.25 M, E_d and E_0 had the highest value. So the films with Zn concentration of 0.25 M were more crystalline. The free carrier concentrations of the films were also calculated. The ZnO thin films with Zn concentration of 0.25 M had the least free charge carrier concentration. Also the real and imaginary part of conductivity is obtained for ZnO thin films considered in this work. The obtained data for void fraction of layers show that by increasing Zn concentration the void fraction of layers had been decreased.

References

1.   M. G. Varnamkhasti, H. R. Fallah and M. Zadsar, *Vacuum* **86** (2012) 871.
2.   A. Farooq and M. Kamran, *Int. J. Appl. Phys. Math.* **2** (2012) 430.
3.   U. Chaitra, D. Kekuda and K. M. Rao, *Ceram. Int.* **43** (2017) 7115.
4.   L. Znaidi, T. Touam, D. Vrel, N. Souded, S. Ben Yahia, O. Brinza, A. Fischer and A. Boudrioua, *Acta Phys. Pol. A* **121** (2012) 165.
5.   O. Gençyılmaz, F. Atay and I. Akyüz, *J. Clean Energy Technol.* **4** (2016) 90.
6.   X. Yu, X. Yu, J. Zhang, D. Zhang, L. Chen and Y. Long, *Sol. Energy* **153** (2017) 96.
7.   V. Musat, A. M. Rego, R. Monteiro and E. Fortunato, *Thin Solid Films* **516** (2008) 1512.
8.   H. Lee, X. Zhang, J. Hwang and J. Park, *Materials* **9** (2016) 851.
9.   M. Kumar, H. Jeong and D. Lee, *J. Alloys Compd.* **720** (2017) 230.
10.   A. Jain, M. Johari, A. Jain, P. K. Pandey and R. Agrawa, *Eng. Technol.* **2** (2013) 3144.
11.   S. Y. Choi, K. Choi and S. J. Kim, *Int. J. Adv. Res. Electr. Electron. Instrum. Eng.* **2** (2013) 6034.
12.   V. Bhardwaj, R. Chowdhury and R. Jayaganthan, *Appl. Surf. Sci.* **389** (2016) 1023.
13.   Z. Y. Alami, M. Salem, M. Gaidi and J. Elkhamkhami, *Adv. Energy, Int. J. (AEIJ)* **2** (2015) 11.
14.   A. U. Moreh, M. Momoh, S. Abdullahi, J. S. Shehu, M. O. Mustapha and N. C. Martha, *J. Multidiscip. Eng. Sci. Technol.* **2** (2015) 2247.
15.   H. K. Juwhari, S. J. Ikhmayies and B. Lahlouh, *Int. J. Hydrog. Energy* **42** (2017) 17741.
16.   K. J. Saji, R. Manoj, R. S. Ajimsha and M. K. Jayaraj, *Adv. Thin-Film Coat. Opt. Appl. III* **6286** (2006) 62860D.
17.   S. Vallejos, F. D. Maggio, T. Shujah and C. Blackman, *Chemosensors* **4** (2016) 1.
18.   C. Periasamy, R. Prakash and P. Chakrabarti, *J. Mater. Sci., Mater. Electron.* **21** (2010) 309.
19.   M. Saleem, L. Fang, H. B. Ruan, F. Wu, Q. L. Huang, C. L. Xu and C. Y. Kong, *Int. J. Phys. Sci.* **7** (2012) 2971.
20.   H. F. Hussein, G. M. Shabeeb and S. Sh. Hashim, *J. Mater. Environ. Sci.* **2** (2011) 423.

21. C. Coşkun, H. Guney, E. Gur and S. Tuzemen, *Turk. J. Phys.* **33** (2009) 49.

22. B. W. Shivaraj, H. N. N. Murthy, M. Krishna and S. C. Sharma, *Int. J. Thin Film Sci. Tec.* **2** (2013) 143.

23. P. Uprety, M. M. Junda, K. Ghimire, D. Adhikari, C. R. Grice and N. J. Podraza, *Appl. Surf. Sci.* **421** (2017) 852.

24. L. Fricke, T. Bontgen, J. Lorbeer, C. Bundesmann, R. Schmidt-Grund and M. Grundmanna, *Thin Solid Films* **571** (2014) 437.

25. M. Gilliot, A. Hadjadj and M. Stchakovsky, *Appl. Surf. Sci.* **421** (2017) 453.

26. S. Peters, Spectra ray and application tutorial, Spectroscopic ellipsometry-theory and application, SENTECH, (2009), pp. 1–32.

27. A. Mendoza-Galván, C. Trejo-Cruz, J. Lee, D. Bhattacharyya, J. Metson, P. J. Evans and U. Pal, *J. Appl. Phys.* **99** (2006) 014306.

28. J. Leng, J. Opsal, H. Chu, M. Senko and D. E. Aspnes, *Thin Solid Films* **313**–**314** (1998) 132.

29. B. V. Rajendra, V. Bhat and D. Kekuda, *Int. J. Emerg. Technol. Adv. Eng.* **3** (2013) 82.

30. N. Chahmat, A. Haddad, A. Ain-Souya, R. Ganfoudi, N. Attaf, M. S. Aida and M. Ghers, *J. Mod. Phys.* **3** (2012) 1781.

31. J. P. Mathew, G. Varghese and J. Mathew, *Chin. Phys. B* **21** (2012) 078104.

32. E. N. Cho, S. Park and I. Yun, *Curr. Appl. Phys.* **12** (2012) 1606.

33. D. A. Ajadi, S. M. Agboola and O. Adedokun, *J. Mater. Sci. Chem. Eng.* **4** (2016) 1.

34. P. Janicek, K. M. Niang, J. Mistrik, K. Palka and A. J. Flewitt, *Appl. Surf. Sci.* **421** (2017) 557.

35. P. Petkova, L. Nedelchev, D. Nazarova, K. Boubaker, R. Mimouni, P. Vasilev, G. Alexieva and D. Bachvarova, *Optik* **139** (2017) 217.

36. M. Sandeep, S. Bhat and S. M. Dharmaprakash, *J. Phys. Chem. Solids* **104** (2017) 36.

37. A. Bakry, *Egypt. J. Solids* **31** (2008) 191.

38. H. Kangarlou, M. Motallebi Aghgonbad and Z. Barjisi, *Optik* **124** (2013) 107.